Climate variability of southern Chile since the Last Glacial Maximum: a continuous sedimentological record from Lago Puyehue (40°S)

Sébastien BERTRAND[1,*], François CHARLET[2], Bernard CHARLIER[3], Virginie RENSON[1] and Nathalie FAGEL[1]

[1] Clays and Paleoclimate Research Unit, University of Liège, B-4000 Liège, Belgium

[2] Renard Centre of Marine Geology, Universiteit Gent, Belgium

[3] Endogenous Petrology and Geochemistry Research Unit, University of Liège, Belgium

Present address: S. Bertrand, Marine Chemistry and Geochemistry, Woods Hole Oceanographic Institution, MS#25, MA 02543, Woods Hole, USA

* Author for correspondence: sbertrand@whoi.edu

Key-words

Sediment, Lake, Grain size, Magnetic susceptibility, Climate, Younger Dryas, South America

Abstract **(221 words)**

This paper presents a multi-proxy climate record of an 11 m long core collected in Lago Puyehue (southern Chile, 40°S) and extending back to 18,000 cal yr BP. The multi-proxy analyses include sedimentology, mineralogy, grain size, geochemistry, loss-on-ignition, magnetic susceptibility and radiocarbon datings. Results demonstrate that sediment grain size is positively correlated with the biogenic sediment content and can be used as a proxy for lake paleoproductivity. On the other hand, the magnetic susceptibility signal is correlated with the aluminium and titanium concentrations and can be used as a proxy for the terrigenous supply. Temporal variations of sediment composition evidence that, since the last glacial maximum, the Chilean Lake District was characterized by 3 abrupt climate changes superimposed on a long-term climate evolution. These rapid climate changes are: (1) an abrupt warming at the end of the last glacial maximum at 17,300 cal yr BP; (2) a 13,100-12,300 cal yr BP cold event, ending rapidly and interpreted as the local counter part of the Younger Dryas cold period, and (3) a 3400-2900 cal yr BP climatic instability synchronous with a period of low solar activity. The timing of the 13,100-12,300 cold event is compared with similar records in both hemispheres and demonstrates that this southern hemisphere climate change lags behind the northern hemisphere Younger Dryas cold period by 500 to 1000 years.

Introduction

Compared to the northern hemisphere, high-resolution paleoclimate studies from the southern hemisphere are still rare despite the fact that this part of the world plays an important role in the understanding of earth climate changes. A key region to study high-resolution climate changes of the southern hemisphere is undoubtedly the southern part of Chile because it has the advantage to be far removed from the northern hemisphere ice sheets and thermohaline circulation influences. Until now, most of the climatic variations evidences since the last glacial maximum (LGM) in southern Chile comes from paleoecological (Heusser et al. 1996, Moreno 1997, 2004, Moreno et al. 1999, 2001, Moreno and Léon 2003) and glacial records (Mercer 1972, Heusser 1990, Lowell et al. 1995, Denton et al. 1999). These data are supplemented by results on marine cores located along the coastal margin (Lamy et al. 2001, 2002, 2004). Until now, little attention has been paid to the sedimentary infilling of the numerous lakes characterizing the Chilean Lake District region (39-43°S). However, lake sediments from many regions of the world have revealed their possibilities to contain high-resolution paleoclimate and paleoenvironmental records (e.g., Colman et al. 1995, Brauer et al. 1999, Chapron et al. 2002, Johnson et al. 2002, Arnaud et al. 2005).

This paper presents a high-resolution sedimentological study of Lago Puyehue during the last 18,000 years. We focus on 3 time periods, for which unresolved key questions still exist in the southern hemisphere: (1) Was the deglaciation uniform or stepwise? (2) Does a cold period similar to the Younger Dryas exist in the southern hemisphere? (3) Was the Holocene a stable climate period? Resolving such paleoclimate questions is important to assess possible inter-hemispheric climate linkages and to deduce the forcing mechanisms of climate changes.

Location and setting

Lago Puyehue (40°40'S, 72°28'W) is located at the foothill of the Cordillera de Los Andes at an elevation of 185 m.a.s.l. (Fig. 1). With a surface of 165.4 km² and a maximum depth of 123 m, it constitutes a typical oligotrophic moraine-dammed lake from the Chilean Lake District (38-43°S; Campos et al. 1989). This lake lies in an overdeepened glacial valley formed during the Quaternary glacial advances (Laugenie 1982). Its catchment covers 1510 km² and is mainly made of Quaternary volcanic rocks covered by several metres of post-glacial andosoils. It is surrounded by several active volcanoes: Puyehue-Cordon Caulle and Casablanca volcanic complexes, peaking at 2240 and 1990 m.a.s.l. respectively. This lake is fed by Rio Golgol to the east, forming the main delta of the lake, and by several smaller rivers (Fig. 1). The outlet of Lago Puyehue (Rio Pilmaiquen) cross-cuts several moraine ridges (Laugenie 1982, Bentley 1997), merges with Rio Bueno and flows into the Pacific westward.

Present-day local climate is characterized by humid temperate conditions with year round precipitation peaking in austral winter (Miller 1976, Heusser 2003). Precipitation is driven by the southern Westerlies and their seasonal shifts. The important topography of the Cordillera de Los Andes forms an effective barrier to the Westerlies and receives most of the precipitation. Annual precipitation increases with elevation and varies between 2000 mm/yr around the lake and 5000 mm/yr on the summit of regional volcanoes (Parada 1973). Mean annual air temperature is 6 to 9°C, with maxima reaching 20°C in January and minima of 2°C in July (Muñoz 1980). This Mediterranean climate is responsible for the development of a dense temperate rainforest (e.g., Moreno and Léon 2003, Moreno 2004). The lake is mainly phosphorous-limited (Campos et al. 1989). Its high silica concentration (15 mg/l; Campos et al. 1989) is characteristic for lakes located in volcanic setting.

Material and Methods

Coring and core processing

In 2001-2002, a coring campaign, using a 3 m-long piston coring system operated from an Uwitec platform, collected a series of 6 cm inner diameter cores in PU-II site (40°41.843'S, 72°25.341'W, depth: 48.4 m; Fig. 1) (De Batist et al. 2006). Core sections were scanned for magnetic susceptibility and gamma-density with a Geotek multi-sensor track on non-opened sections. Cores were then opened and sediment texture was described (colour, grain size, structure, contacts). Whole core magnetic susceptibility was re-measured for higher resolution on open sections with a Bartington MS2E point sensor every 5 mm. The 3 m long sections were then correlated using magnetic susceptibility results and remarkable layers described macroscopically (Fig. 2). An 11.22 m long composite core was constructed. The working half of the composite core was sub-sampled in 1 cm thick slices. After U-channel sampling, the archive half was devoted to thin-sections preparation.

Methods

The methods applied on PU-II long core hereafter have been selected from a preliminary high-resolution and pluri-methodological study carried out on a short core from PU-II site spanning the last 600 years (Bertrand et al. 2005).

Grain size measurements were performed on bulk sediment using a laser diffraction particle analyser Malvern Mastersizer 2000 detecting a 0.02 to 2000 µm size range. Samples were introduced into a 100 ml desionised water tank free of additive dispersant, split with a 2000 rpm stirrer and crumbled with ultrasonic waves. Sample quantity was adjusted in order

to obtain a laser beam obscuration between 10 and 20 %. Grain size parameters are averaged over 10,000 scans. Distribution parameters have been calculated following Folk and Ward (1957). Grain size analyses were realised with a 5 mm sampling step between 0 and 430 cm and then every 2 cm between 430 and 1122 cm.

Loss-on-ignition (LOI) was measured after 24h at 105°C (LOI_{105}), after 4h at 550°C (LOI_{550}) and after 2h at 950°C to estimate water content, organic matter content and inorganic carbonate content, respectively (Heiri et al. 2001). Because LOI_{550} is dependent on the sample weight (Heiri et al. 2001), we always used 1g of dry samples (0.97 ± 0.07 g). A good correlation between LOI_{550} and TOC ($r = 0.95$) has been calculated for recent sediments of Lago Puyehue, making LOI_{550} data very significant (Bertrand et al. 2005).

Bulk mineralogy was achieved by X-ray diffraction (XRD) on a Bruker D8-Advance diffractometer with CuKα radiation. Bulk samples were powdered to 100 µm using an agate mortar. An aliquot was separated and mounted as unoriented powder by the back-side method (Brindley and Brown 1980). The powder was scanned by XRD between 2° and 45° 2θ. The data were analysed in a semi-quantitative way following Cook et al. (1975).

Clay mineralogy was established on the < 2 µm fraction obtained after 50 min of sedimentation (Stokes's settling law). Oriented mounts were realised by the "glass-slide method" (Moore and Reynolds 1989) and subsequently scanned on the diffractometer. Slides containing crystallised clays after air drying (N) were also scanned after ethylene-glycol solvation during 24h (EG) and after heating at 500°C during 4h (500). Since amorphous clays are abundant in the samples, we estimate the crystallised clay content using the intensity of the most intense clay diffraction peak on the natural (N) diffractogram.

Major elements of PU-II long core were determined by X-ray fluorescence (XRF) on Li-borate glass after loss-on-ignition at 950°C. Analyses were performed on an ARL 9400.

Accuracy is 0.50 %, 3.07 % and 1.69 % for SiO_2, TiO_2 and Al_2O_3 respectively (Bologne and Duchesne 1991). Biogenic silica is deduced by normative calculation (Leinen 1977):

$$\text{bio-}SiO_2 = SiO_2 \text{ tot} - x \cdot Al_2O_3$$

where x is the SiO_2/Al_2O_3 ratio of terrigenous sediments. When normalizing with Al, we assume that all Al derives from detrital material, and that the detrital material has a constant Si/Al ratio. Soils and rocks in the lake catchment represent the main sources of lacustrine detrital particles. Their SiO_2/Al_2O_3 ratio was calculated by XRF analyses (mean: 3.5; see Bertrand et al. 2005). The two biogenic silica negative modelled values have been set to zero (170 cm: -1.3 and 382 cm: -1.5). Results obtained by this method are close to results obtained by alkaline extraction (Bertrand et al. 2005).

Except for grain size and magnetic susceptibility, all analyses were performed on a 1cm thick sample selected every 10 cm, avoiding samples containing macroscopically visible tephra layers and turbidites. Samples below tephra layers were preferred in order to discard a possible tephra influence on the sediment composition.

Core sedimentology and chronology

Lithology

The sediment is made of finely laminated to homogeneous brown silty particles (Fig. 2). According to smear slides observation, the sediment is mainly composed of diatoms, organic matter, amorphous clays, crystallised minerals and volcanic glasses throughout the core. Sponge spicules are secondary constituents. Diatom assemblages are dominated by *Cyclotella stelligera* and *Aulacoseira granulata* (Sterken et al. 2006b). Seventy-eight tephra layers, coarse-grained, embedded in a fine matrix and generally less than 1 cm thick, were

macroscopically described. Their total thickness is 52.3 cm. The thickest tephra occurs at 102.3-109.8 cm depth. They have been deeply investigated in terms of tephrostratigraphy (Juvigné et al. unpublished data). Moreover, several ~ 1 cm thick grey or greenish clay layers often containing pumice pebbles were observed. They are interpreted as a result of the in situ weathering of pumice deposits. Three turbidites layers are macroscopically observed, at 379.5-381, 396.5-397.25 and 956-971 cm. This macroscopical interpretation was later supported by grain size analyses and thin-sections observation.

Chronology

The age-depth model was realised using 9 AMS radiocarbon datings on bulk sediment realised at Poznan Radiocarbon Laboratory (Czernik and Goslar 2001). Radiocarbon dates were calibrated with BCal using atmospheric data of Stuiver et al. (1998) and we used the weighted average of each calibrated date to perform the age-depth model (Table 1). The date obtained at 1119 cm was rejected because of its stratigraphic inconsistency with other dates. This choice was supported by the very low carbon content of this sample (0.4 mg), making the result less reliable. Moreover, we used two tephra layers dated by varve counting as chronostratigraphic markers (Boës and Fagel 2006). These tephras originate from historical volcanic eruptions of Puyehue Volcano and Cordon Caulle (AD 1921-1922) and Osorno Volcano (AD 1575) (Boës and Fagel 2006). We consider the 78 tephra layers and the 3 turbidites as instantaneous deposits and take it into account during the realisation of the age-depth model (Fig. 3). No continuous age-depth model was able to fully reproduce the ^{14}C distribution (cubic splines and polynomial with up to 8 terms were tested). We thus use a discontinuous age-depth model assuming constant sedimentation rates in 4 domains for which

linear regressions on ^{14}C datings were calculated. The resulting temporal sampling resolution (10 cm) varies between 63 and 278 yrs with a mean of 162 yrs.

Results

Mineralogy and physical proxies (Fig. 4)

Bulk mineralogy shows the occurrence of amorphous particles (75 %), plagioclases (17 %), pyroxenes (7 %) and traces of quartz (< 2 %). As revealed by smear slides observation, amorphous particles are made of biogenic silica, volcanic glasses, amorphous clays and organic matter. The < 2 μm fraction is mainly made of amorphous clays, i.e., allophane as demonstrated by IR spectra and chemical analyses. It is typical of weathering products in volcanic environments. Several samples display an additional peak at 14.5 Å. This peak shifts to 16.5 Å after ethylene glycol solvation but not with glycerol and collapses into a broad diffraction band between 14 and 9.5 Å by heating above 200°C. Such behaviour is typical for a hydroxy-interlayered vermiculite. Its occurrence is not significant, except below 780 cm where it occurs in combination with allophane.

Magnetic susceptibility (MS) data vary between 43.10^{-6} S.I. (9.5 cm) and 1277.10^{-6} S.I. (233 cm) (mean: 187 ± 113.10^{-6} S.I.). We observe a gradual increase of MS from 0 to 150 cm and an important shift at 815 cm. Higher values correspond to tephra layers. Because of the paleoclimate purpose of this research, tephra-related MS peaks were removed from the database.

Water content of sediment (LOI_{105}) ranges from 75.7 % to 31.3 % (mean: 56.1 ± 7.8). An important shift to lower values (~ 50 %) occurs at 805 cm. Between 60 and 805 cm,

values are close to ~ 60 % except several peaks close to 40 %. Values demonstrate a decreasing trend for the first 60 cm.

LOI_{550} values range between 2.35 and 10.23 % with a mean of 5.73 ± 1.84 %. Higher values are observed in the upper 50 cm, while lower values occur at the base of the core, below 810 cm. LOI_{950} data are very low and not significant (1.13 % ± 0.38) because the sediment does not contain any inorganic carbonate. Small LOI_{950} values are due to weight loss by residual organic matter and loss of clays structural water (Heiri et al. 2001).

The mean grain size data range from 2.29 to 390 µm. Extreme values are due to tephra layers (coarse grain size) and upper part of turbidites (fine grain size). After removal of event deposits (tephras and turbidites), the means range from 2.52 to 27.49 µm, with a mean of 12.45 ± 3.89 µm. An important shift occurs at 810 cm. Below this level (810-1122 cm), mean grain size ranges around 8.74 µm. Between 42 and 805 cm, sediment is coarser (mean 12.49 µm). The highest values occur between 7 and 25 cm (14.54-27.49 µm).

Geochemical data (Fig. 5)

Biogenic silica content of the sediment ranges from 0.0 % to 43.7 %. The mean bio-SiO_2 content of sediment is 15.1 ± 9.1 %. The highest values occur at 20 and 590 cm (43.4 and 43.7 %, respectively) whereas samples are free of biogenic silica at 170 and 382 cm. An important shift occurs in the 800-830 cm interval.

Aluminium (Al_2O_3) and titanium (TiO_2) concentrations vary from 9.51 to 17.8 % (mean: 14.4 ± 1.51 %) and from 0.54 to 1.26 % (mean: 0.82 ± 0.14), respectively. For both elements, the lower values are observed at 20 cm (Al_2O_3: 9.55 % and TiO_2: 0.54 %) and 590 cm (Al_2O_3: 9.51 % and TiO_2: 0.54 %). For aluminium, the higher concentrations occur at 170

cm (17.31 %) and 382 cm (17.79 %). For titanium, higher values occur below 810 cm and are maximum at 950 cm (1.26 %). Both elements show a shift in the 800-830 cm interval.

Discussion

Detrital sediment origin and weathering

The bulk mineralogical data (Fig. 4) reveal a high content of amorphous particles, overestimated by the significant biogenic fraction occurring in lake sediments (biogenic silica and organic matter). The abiogenic mineralogy is close to the mineralogy of regional andosoils, which constitute the main sedimentary detrital source. These soils are rich in volcanic glasses and allophane, a typical amorphous clay mineral produced by weathering of volcanic glasses and plagioclases.

Allophane is the only clay mineral occurring in regional andosoils. No occurrence of imogolite, a recrystallisation product of allophane, has been evidenced. In the PU-II long core, hydroxy-interlayered vermiculite (HIV) occurs in addition to allophane, mainly below 780 cm. Its origin is ambiguous. HIV frequently originates from weathering of chlorite, itself inherited from hornblende, biotite or other ferro-magnesian minerals (Barnhisel 1977). However, in sediments from Lago Puyehue, including tephra layers, and in regional soils, biotite has never been observed and amphibole (hornblende) is rare. The only ferro-magnesian mineral occurring in local soils is pyroxene (Laugenie 1982). Consequently, the HIV is probably the end product of the following weathering sequence: pyroxene → chlorite → HIV. The intermediate chlorite (green clay mineral) agrees for the green colour characterizing the samples containing HIV. The occurrence of this weathering product below 780 cm probably reflects high precipitation during this period but can also be due to a change in the relative

content of ferro-magnesian minerals in the volcanic rocks occurring in the watershed. This hypothesis agrees with the evolution of Fe_2O_3 and MgO content of lavas emitted from Puyehue-Cordon Caulle (Gerlach et al. 1988). Indeed, Fe_2O_3 and MgO content of late glacial lavas (8.84 % and 5.92 %, respectively) are higher than those of post-glacial lavas (6.37 % and 1.41 % respectively).

Relationships between proxies and their paleoenvironmental significance

We use aluminium and titanium concentrations to trace the terrigenous fraction of the sediment. Biogenic silica and LOI_{550} represent its biogenic content.

Before interpreting the biogenic contents, one must be aware of the difference between the preserved biogenic fraction compared to the original productivity. The biogenic silica fraction of sediment represents the siliceous skeletal matter from the epilimnion, minus the dissolution that occurs during settling in the water column and on the lake floor (Cohen 2003). Assuming that dissolution is proportional to primary biogenic production, biogenic silica can be interpreted in terms of lake paleoproductivity. In Lago Puyehue, the biogenic silica content reflects the abundance of diatoms in lake sediments. It is mainly controlled by the *Aulacoseira* concentration (Sterken et al. 2006b). Smear slide observation has revealed that diatoms are abundant and well preserved throughout the core. Other sources of biogenic silica (e.g., sponge spicules and phytolithes) are rare. In volcanic settings, one may expect an influence of volcanic eruptions on lake productivity (Lotter et al. 1995, Barker et al. 2000). Results on Puyehue samples have shown that there is no relation between the biogenic silica content and the distance to the closest tephra ($r^2 = 0.003$), suggesting that, in Lago Puyehue, volcanic eruptions do not have any influence on lake productivity (Sterken et al. 2006a).

Organic matter content of the sediment includes both allochtonous and autochtonous components. For the last 600 years, C/N analyses have demonstrated that organic matter mainly originates from in-lake productivity (Bertrand et al. 2005). We consider this assumption valid for the whole PU-II long core. Moreover, organic matter preservation in the sediment is influenced by remineralization process during early diagenesis. This leads, for the upper sediments, to a diagenetic profile showing a decreasing organic matter content with depth (Zimmerman and Canuel 2002). Aware of these early changes, biogenic silica and organic matter concentrations can be used as proxies of lake productivity.

From figures 4 and 5, we clearly observe relationships between independent proxies. Al_2O_3, TiO_2 and MS show a strikingly similar behaviour. On the other hand, LOI_{105}, LOI_{550}, grain size and bio-SiO_2 seem to covary. To further investigate relationships between variables, correlation coefficients were calculated and a principal component analysis (PCA) was performed (Table 2, Fig. 6). Regarding the PCA analysis, F1 axis explains 71.61 % of the variability and the analysis demonstrates the occurrence of 2 data groups. The first association is made of Al_2O_3, TiO_2 and MS. The second group is made of LOI_{105}, LOI_{550}, mean grain size and biogenic silica. These two data groups are strongly inversely correlated arguing for a two end-member system made of (1) terrigenous and (2) biogenic particles.

Terrigenous particles

Al_2O_3 and TiO_2 are positively correlated ($r = 0.68$) and used as markers of the terrigenous fraction of the sediment. These elements mainly originate from regional andosoils by river discharge. The relatively high mean MS values are due to the volcanic geological context, responsible of a high percentage of magnetic minerals in the sediment. Because magnetic minerals are contained in the terrigenous fraction of the sediment, the MS signal clearly reflects the detrital supply (Arnaud et al. 2005), as shown by its positive correlation with

Al_2O_3 (r = 0.53) and TiO_2 (r = 0.37). Down core variations of the MS signal can thus be used to infer variations in the terrigenous supply. These variations are mainly linked to precipitation, but, in the highly active volcanic context of the area, the rejuvenation of the erodible volcanic material by volcanic eruptions may also influence the terrigenous supply.

Biogenic particles

Biogenic silica and LOI_{550} represent the siliceous organisms and organic matter preserved in the sediment, respectively. These two parameters are positively correlated (r = 0.62) and are assumed to represent the overall lake paleoproductivity. The PCA analysis (Fig. 6) and correlation coefficients (Table 2) demonstrate that LOI_{105} and grain size are positively correlated with these parameters. LOI_{105} variations are closely linked to lithological changes, i.e., diatoms and organic mater content, because their ability to retain water compared to the terrigenous sediment. Variations of LOI_{105} are thus related to changes in the biogenic content of the sediment. Similarly, a close relation between grain size and biogenic silica (r = 0.71) and LOI_{550} (r = 0.67) is observed. The coarser the sediment, the higher the biogenic content is. This relation is due to the coarse size of diatoms and organic matter. Indeed, the bulk grain size distribution can be decomposed in two fractions (Fig. 7): the fine terrigenous sediments and the coarse biogenic fraction, mainly made of diatoms, but also vegetal tissue remains. This result is comforted by the size of diatoms (20-60 µm) deduced from smear slides observation. A coarse grain size thus reflects a high biogenic content and can be interpreted as a high lake paleoproductivity.

Because MS and grain size data were measured at high resolution, these signals can be used for tracing relative changes in terrigenous and biogenic components.

Climate variability since the last glacial maximum

Generally, discussion about lake sediments must consider changes in proxies by mass accumulation rates (MAR). However, during the major proxy variations of PU-II core, e.g., mainly between 700 and 1122 cm (9750-17900 cal yr BP), the age-depth model is linear suggesting that contents (weight %) and MAR have similar trends (Fig. 8). For periods younger than 9000 cal yr BP, MAR calculation is biased by the age-depth model shape. Indeed, age-depth modelling with linear regression induces breakpoints in the total sedimentation rate, not reflecting natural changes in the sediment accumulation. Thus, MARs were only calculated between 18,000 and 9000 cal yr BP (Fig. 8).

In lake environments, increased productivity is controlled by nutrient availability, light and temperature. The solar energy plays a direct role in the productivity of these lakes at a seasonal scale but is considered globally constant at a larger time-scale. Therefore, we interpret paleoproductivity variations due to temperature and/or nutrient supply changes. The choice between both can be deduced from the parallelism with the detrital supply results. We interpret high detrital supply as reflecting an higher catchment erosion, linked to increased precipitations.

The temporal distribution of sediment composition, mean grain size and magnetic susceptibility reveals 7 periods (zones A to G), reflecting changes in productivity and rate of detrital supply during the last 18,000 years (Fig. 8).

Before 17,300 cal yr BP (zone A), the sediment is mainly composed of terrigenous particles (90 %) reflecting the very low bio-SiO_2 MAR and accounts for a very low lake paleoproductivity. This period is interpreted as cold and humid. The end of this period is marked by an abrupt increase of lake paleoproductivity at 17,300 cal yr BP. This is interpreted as the result of a warming pulse, enhancing lake plankton development and probably marking

the end of the last glacial. A change in the lake stratification, from cold monomictic during glacial times to warm monomictic after 17,300 cal yr BP, could also explain the abrupt biogenic silica increase at 17,300 cal yr BP (Sterken et al. 2006b). The decrease of the terrigenous supply at 17,300 cal yr BP probably reflects a slightly drying climate. This abrupt climate change is followed by a progressive cooling, deduced from the decreasing content in biogenic particles and in grain size data until 13,100 cal yr BP (zone B). This general shape (abrupt warming at 17,300 cal. BP followed by a gradual cooling during thousands of years) is strikingly similar to the behaviour of the D/O event 1 described in Greenland ice cores (Grootes et al. 1993). In zone B, the terrigenous supply increases at 15,000-12,500 cal yr BP, reflecting a strengthening of precipitation. The most outstanding feature of low paleoproductivity occurs in the zone C_1, between 13,100 and 12,300 cal yr BP, delimitating one of the coolest periods between the last glacial maximum (LGM) and present. All the proxies agree with a cold climate.

The end of this period is marked by a gradual warming between 12,300 and 11,800 cal yr BP (zone C_2). Before 13,300 cal yr BP (zones A to C), terrigenous particles MAR remains globally high (300-400 $g \cdot m^2/yr$) reflecting significant precipitation in the watershed and/or low vegetation cover enhancing high sediment availability. Terrigenous MAR decreases during the zone C_2 until values of ~ 200 $g \cdot m^2/yr$, contemporaneously with the bio-SiO_2 MAR increase. This reflects a warming and drying climate at the beginning of the Holocene.

Between 11,800 and 7800 cal yr BP (zone D), paleoproductivity reaches its maximum and terrigenous MAR are low, reflecting high temperatures and low precipitation in the early Holocene. Similar conclusions are also obtained from paleoecological proxies (Sterken et al. 2006b, Vargas et al. 2006). Higher organic matter productivity is recorded since ~ 10,000 cal yr BP (Fig. 7). It is probably induced by the development of the vegetation in the lake catchment, due to favourable climate conditions (Vargas et al. 2006).

After 7800 cal yr BP, paleoproductivity slightly decreases and remains rather high until the second part of the last millennium (zones E to G). Two exceptions to this general trend are: (1) the high variability of paleoproductivity between 6000 and 3500 cal yr BP and (2) a cold and/or humid event occurring between 3400 and 2900 cal yr BP. Both its initiation and its end are abrupt. Finally, the last 600 years sediments have been investigated at higher resolution (Bertrand et al. 2005) and show that the recent lake infilling history is mainly driven by changes in the detrital MAR reflecting an increase in precipitation at the onset of the Little Ice Age.

Regional and southern-hemisphere implications

Our results on Lago Puyehue sediments generally agree with previous sedimentological, paleoecological and glacial studies from the Chilean Lake District (Lowell et al. 1995, Heusser et al. 1996, Moreno et al. 1999, 2001, Moreno and Léon 2003, Moreno 2004), Chiloé Island (Abarzúa et al. 2004) and northern Argentinan Patagonia (Ariztegui et al. 1997, Hajdas et al. 2003). Most of these climate interpretations are summarized in McCulloh et al. (2000). In order to demonstrate the regional or hemispheric validity of climate change results inferred from Lago Puyehue sediments, we made comparisons with regional data from literature. The following discussion focuses on four important climate change periods: (1) the rapid warming transition at 17,300 cal yr BP; (2) the very cold climate period between 12,300 and 12,800 cal yr BP and its onset; (3) the climate optimum during the early Holocene and (4) the cold/wet event recorded at 3400-2900 cal yr BP.

(1) Our data demonstrate a rapid shift of paleoproductivity at ca. 17,300 cal yr BP, interpreted as an abrupt warming. It probably marks the end of the last glacial maximum (LGM). Both glacial and paleoecological studies from the Chilean Lake District confirm these

results. Paleoecological data demonstrate a sudden rise in temperature that initiated deglaciation synchronously over 16°S of latitude at 17,500-17,150 cal yr BP (McCulloh et al. 2000). During the end of the last glacial phase (19,600-17,500 cal yr BP), a forest made of cold-resistant North-Patagonian species, characteristic of cold and hyperhumid conditions (~ 4000 mm/yr), was present at 40°S (Moreno 1997, Moreno and Léon 2003). At 17,500 cal yr BP, this forest was rapidly replaced by a North-Patagonian evergreen rainforest, demonstrating a 5 to 7°C warming (Lowell et al. 1995, Heusser et al. 1996, 1999, Moreno 1997, Moreno et al. 1999). This abrupt climate change is followed by an important withdrawal of the Andean piedmont glaciers at 16,800 cal yr BP (Lowell et al. 1995). At this time, sea surface temperature off Chile was already rising since ~ 1500 years (Lamy et al. 2004). This scenario is inconsistent with Bentley's (1997) deglaciation story of Lago Puyehue. According to his radiocarbon data, the deglaciation of Lago Puyehue was only complete by ~ 14,750 cal yr BP.

(2) After the rapid warming that happens at 17,300 cal yr BP, our data demonstrate a gradual climate cooling until 12,300 cal yr BP, with slightly higher precipitations during the 15,000-12,500 cal yr BP interval. Paleoecological data demonstrate that the warming between 17,500 cal yr BP and the beginning of the Holocene was gradual (Bennett et al. 2000) or punctuated by several cooling phases (Moreno et al. 2001, Moreno and Léon 2003).

For several decades, the existence of a possible Younger Dryas in the Chilean Lake District has been a controversial topic (Mc Culloh et al. 2000). According to our results, Lago Puyehue paleoproductivity reaches its minimum during the 13,100-12,300 cal yr BP interval. It was followed by a 500 year warming climate, reaching an optimum at the beginning of the Holocene close to 11,800 cal yr BP. We interpret the 13,100 - 12,300 cal yr BP interval as a cold period marking the last deglaciation. It acts as the Chilean Lake District counter part of the northern hemisphere Younger Dryas. Neither paleoecological nor glacial studies from the

Chilean Lake District clearly suggest a cold period during the Younger Dryas. The only proof for such a cold period during the Younger Dryas chronozone are from Heusser et al. (1999), Moreno (1997) and Moreno et al. (2001). However, the presence of charcoal at this period in many profiles complicates the interpretation (e.g., Moreno et al. 1999, 2001, Moreno 2000). From paleoecological studies, Heusser et al. (1999) demonstrate a cold period between 14,450 and 11,400 cal yr BP. From three Chilean Lake District sites, Moreno (1997) and Moreno et al. (2001) indicate a cooling event at 13,475 cal yr BP followed by a warming pulse at 11,200 cal yr BP. These authors consider climate changes in meridional Chile in agreement with those of the northern hemisphere. These results strikingly contrast with the interpretation of Bennett et al. (2000), arguing for a climate stability during the last glacial-Holocene transition in Chile, deduced from the apparent vegetation homogeneity they found in pollen records between 16,800 and 7840 cal yr BP between 44 and 47°S. Sea surface temperature reconstructed from the study of alkenones on a marine core from the Chilean margin at the same latitude does not contain any evidence of a Younger Dryas cold period (Lamy et al. 2004). In the Chilean Lake district, no re-advance of Andean glaciers has been evidenced during this period (Andersen et al. 1995, Lowell et al. 1995). In Patagonia, a Younger Dryas cooling event has not been recorded (Glasser et al. 2004). However, on the eastern side of the Andes, Ariztegui et al. (1997) described a Younger Dryas advance of the Tronador ice-cap (Argentina, 41°S) reflected in Lago Mascardi sediments between 13,475 and 12,000 cal yr BP. This cold event recorded in Lago Mascardi was further confirmed by an intensive dating program conducted by Hajdas et al. (2003). According to these results, both the Huelmo (Chile) and Lago Mascardi (Argentina) sites recorded a cold event close to the Younger Dryas chronozone. This event, locally named the Huelmo/Mascardi cold reversal, begun at 13,475 cal yr BP and ended at 12,000 cal yr BP (Hajdas et al. 2003). Its onset precedes the onset of the northern hemisphere Younger Dryas by 550 years (Hajdas et al. 2003). Our results agree

with the timing and magnitude of the Huelmo/Mascardi cold reversal, but the duration of the cold period recorded in Lago Puyehue sediments seems ~ 600 years shorter. The Huelmo/Mascardi cold reversal would be the regional counterpart of the northern hemisphere Younger Dryas, preceding it by 500 to 1000 years. The Antartic Cold Reversal recorded in Vostok and Byrd ice cores is in agreement with a 1000 years lag of the southern hemisphere climate changes compared to those of the northern hemisphere (Blunier et al. 1998). This could be explained by the Southern Ocean flywheel role in northern hemisphere climate changes during the last deglaciation (Knorr and Lohmann 2003).

(3) Paleoproductivity of Lago Puyehue reaches its maximum, close to present-day values, during the first part of the Holocene between 11,800 cal yr BP and 7800 cal yr BP. Moreover, this period is characterized by a low terrigenous supply and is interpreted as warm and dry, reflecting an early Holocene climate optimum. These results are consistent with palynological data from the Chilean Lake District and Chiloé Island (Moreno and Léon 2003, Abarzúa et al. 2004, Moreno 2004). Huelmo and Lago Condrito (41°S) records reveal warm and dry climate conditions between 12,200 and 7700 cal yr BP and 11,000-7600 cal yr BP, respectively (Moreno and Léon 2003, Moreno 2004). The same pattern was interpreted on Chiloé Island (43°S), arguing for a warmer and drier than present-day climate between 11,400 and 7840 cal yr BP (Abarzúa et al. 2004). A similar warm/dry phase is recorded in central Chile (Laguna Aculeo, 34°S) during the early to mid Holocene period (9500-5700 cal yr BP) (Jenny et al. 2002). This period is interpreted as a poleward shift of the Westerlies (Moreno and Léon 2003). From these results, it is clear that the early Holocene in the Chilean Lake District is characterized by a climatic optimum (warm and dry) which probably extended further north.

(4) The relatively temperate Holocene climate is punctuated by a very low productive and/or high terrigenous supply event lasting a maximum of 500 years. In Lago Puyehue

sediments, this event is recorded between 3400 and 2900 cal yr BP. From sedimentological data, we cannot decipher if this event was cold, humid or both. Pollen and diatom analyses do not show any similar event (Sterken et al. 2006b, Vargas et al. 2006). Contemporaneously, late Holocene glacial advances related to moisture increase were recorded in northern Chile at 29°S (Grosjean et al. 1998). Additional evidence exists in South America and in many places of the world (van Geel and Renssen 1998, van Geel et al. 2000). In Chile, paleoecological analyses do not reveal abrupt climate changes during this period. Moreover, marine sediments demonstrate a continuous paleoproductivity throughout the last 8000 years (Lamy et al. 2002) and do not show any climate disturbance close to 3000 cal yr BP. An accurate dating of this event by radiocarbon is difficult because of the plateau in the calibration curve characterizing this period. According to van Geel et al. (2000), rapid climate changes at this period are due to a decreasing solar activity.

Conclusion

Lago Puyehue contains a continuous record of lake productivity and sediment supply during the last 18,000 calendar years. These variations are related to changes in temperature and precipitations, respectively. Three main abrupt climate changes are recorded.

(1) A warming and drying climate at 17,300 cal yr BP, characterizing the end of the last glacial maximum. This reflects a warming pulse of 5 to 7°C.

(2) A temperature minimum during the 13,100-12,300 interval. This event is the local counterpart of the northern hemisphere Younger Dryas and is known as the Huelmo/Mascardi cold reversal. Its onset precedes the northern hemisphere Younger Dryas by ~ 500 years. Moreover, the Antartic cold reversal recorded in Vostok and Byrd ice cores lag the northern

hemisphere Younger Dryas by ~ 1000 years, supporting the fact that the Southern Ocean can be the flywheel of northern hemisphere climate changes.

(3) A short and abrupt cold/humid period during the 3400-2900 cal yr BP interval. This period is linked to glacial advances in the central Andes, probably due to a minimum in the solar activity.

These three abrupt climate changes are superimposed on millennial time scale climate variations. From 17,300 to 12,300 cal yr BP, the Chilean Lake District is characterized by a gradual decrease in temperatures, while precipitation was particularly high before 17,300 and during the 15,000-13,000 interval. The early Holocene is characterized by a warm and dry climate. After 7800 cal yr BP, the Chilean Lake District climate does not vary significantly. Finally, high lake paleoproductivity is recorded in the last 500 years.

Past changes in precipitation in the Chilean Lake District suggest latitudinal shifts in the position and strength of the southern Westerlies. Before the initiation of the Holocene at 11,800 cal yr BP, the southern Westerlies were significantly influencing the Chilean Lake District climate, with a small poleward shift between 17,300 and 15,000 cal yr BP. The warm and dry phase between 11,800 and 7800 cal yr BP could be related to a significant poleward shift of the southern Westerlies, close to its actual position.

Acknowledgments

This research is supported by the Belgian OSTC project EV/12/10B "A continuous Holocene record of ENSO variability in southern Chile". We would like to acknowledge Mario Pino, Maria Mardones and Roberto Urrutia for their fieldwork assistance during our 2001-2002 mission in Chile. Thanks to Christian Beck, Marc Tardy, Fabien Arnaud, Vincent Lignier (LGCA, Chambery), Xavier Boës (ULg), Waldo San Martin and Alejandro Peña (EULA, Chile) for lake coring and to Jean-Jacques Garroi for its substantial help in improving statistical analyses. We thank the GFZ research centre (H. Oberhänsli, Germany), the Chemical department of the University of Liège (A. Rulmont) and the EAWAG research institute (M. Sturm, Switzerland) for proving kind access to Geotek, particle sizer and Bartington magnetic susceptibility meter respectively. Thanks to M. Sterken (U. Gent) for the numerous fruitful discussions on the biological aspect of Lago Puyehue limnology. M. De Batist and M.-F. Loutre have improved an earlier version of this manuscript.

References

Abarzúa A.M., Villagrán C. and Moreno P.I. 2004. Deglacial and postglacial climate history in east-central Isla Grande de Chiloé, southern Chile (43°S). Quat. Res. 62: 49-59.

Andersen B. G., Denton G. H., Heusser C. J., Lowell T. V., Moreno P. I., Hauser A., Heusser L. E., Schlüter C. and Marchants D. R. 1995. Climate, vegetation and glacier fluctuations in Chile, between 40°30' and 42°30'S latitude - a short review of preliminary results. Quat. Int. 28: 199-201.

Ariztegui D., Bianchi M.M., Masaferro J., Lafargue E. and Niessen F. 1997. Interhemispheric synchrony of Late-glacial climatic instability as recorded in proglacial Lake Mascardi, Argentina. J. Quat. Sci. 12: 333-338.

Arnaud F., Revel-Rolland M., Chapron E., Desmet M. and Tribovillard N. 2005. 7200 years of Rhône river flooding activity in Lake Le Bourget: A high resolution sediment record of NW Alps hydrology. The Holocene 15: 420-428.

Barker P., Telford R., Merdaci O., Williamson D., Taieb M., Vincens A. and Gibert E. 2000. The sensitivity of a Tanzanian crater lake to catastrophic tephra input and four millenia of climate change. The Holocene 10: 303-310.

Barnhisel R.I. 1977. Chlorites and Hydroxy Interlayered Vermiculite and Smectite. In: Dixon JB, Weed SB, Kittrick JA, Milford MHWhite JL (eds). Minerals in soil environments. Soil Science Society of America, Madison, Wisconsin, pp. 331-356.

Bennett, K.D. 1994. 'psimpoll' version 2.23: A C program for analysing pollen data and plotting pollen diagrams. INQUA Working Group on Data Handling Methods Newsletter 11: 4-6.

Bennett K.D., Haberle S.G. and Lumley S.H. 2000. The Last Glacial-Holocene Transition in Southern Chile. Science 290: 325-328.

Bentley M.J. 1997. Relative and radiocarbon chronology of two former glaciers in the Chilean Lake District. J. Quat. Sci. 12: 25-33.

Bertrand S., Boës X., Castiaux J., Charlet F., Urrutia R., Espinoza C., Charlier B., Lepoint G. and Fagel N. 2005. Temporal evolution of sediment supply in Lago Puyehue (Southern Chile) during the last 600 years and its climatic significance. Quat. Res. 64: 163-175.

Blunier T., Chappellaz J., Schwander J., Dälenbach A., Stauffer T.F., Stocker T.F., Raynaud D., Jouzel J., Clausen H.B., Hammer C.U. and Johnsen S.J. 1998. Asynchrony of Antarctic and Greenland climate change during the last glacial period. Nature 394: 739-743.

Boës X. and Fagel N. 2006. Relationships between southern Chilean varved lake sediments, precipitation and ENSO for the last 600 years. J. Paleolimnol.

Bologne G. and Duchesne J.-C. 1991. Analyse des roches silicatées par spectrométrie de fluorescence X : précision et exactitude. Professional Paper of the Belgian Geological Survey. Brussels. 11 p.

Brauer A., Endres C., Günter C., Litt T., Stebich M. and Negendank J.F.W. 1999. High resolution sediment and vegetation responses to Younger Dryas climate change in varved lake sediments from Meerfelder Maar, Germany. Quat. Sci. Rev. 18: 321-329.

Brindley, G. W. & Brown, G. 1980. Crystal structures of clay minerals and their x-ray identification. Mineralogical Society Monograph, London, Vol. 5. 495 p.

Bronk Ramsey C. 2001. Development of the Radiocarbon program OxCal. Radiocarbon 43(2A): 355-363.

Campos H., Steffen W., Agüero G., Parra O. and Zúñiga L. 1989. Estudios limnologicos en el Lago Puyehue (Chile): morfometria, factores fisicos y quimicos, plancton y productividad primaria. Med. Amb. 10: 36-53.

Chapron E., Desmet M., De Putter T., Loutre M.F., Beck C. and Deconinck J.F. 2002. Climatic variability in the northwestern Alps, France, as evidenced by 600 years of terrigenous sedimentation in Lake Le Bourget. The Holocene 12: 59-68.

Charlet F., De Batist M., Chapron E., Bertrand S., Pino M. & Urrutia R. 2006. Seismic-stratigraphy of Lago Puyehue (Chilean Lake District): new views on its deglacial and Holocene evolution. J. Paleolimnol.

Cohen A.S. 2003. Paleolimnology: the history and evolution of lake systems. New York: Oxford University Press. 528 p.

Colman S.M., Peck J.A., Karabanov E.B., Carter S.J., Bradbury J.P., King J.W. and Williams D.F. 1995. Continental climate response to orbital forcing from biogenic silica records in Lake Baikal. Nature 378: 769-771.

Cook H.E., Johnson P.D., Matti J.C. and Zemmels I. 1975. Methods of sample preparation and x-ray diffraction data analysis, x-ray mineralogy laboratory. In: Kaneps AG (eds). Initial reports of the DSDP, Washington DC, pp. 997-1007.

Czernik T. and Goslar T. 2001. Preparation of graphite targets in the Gwilice radiocarbon laboratory for AMS ^{14}C dating. Radiocarbon 43(2): 283-291.

De Batist M., Fagel N., Loutre M.F. and Chapron E. 2006. A 17,900 year multi-proxy lacustrine record of Lago Puyehue (Chilean Lake District): Introduction. J. Paleolimnol.

Denton G.H., Heusser C.J., Lowell T.V., Moreno P.I., Andersen B.G., Heusser L.E., Schlüter C. and Marchant D.R. 1999. Geomorphology, stratigraphy, and radiocarbon chronology of Llanquihue drift in the area of the southern lake district, seno reloncaví, and isla grande de Chiloé, Chile. Geog. Ann. 81 A(2): 167-212.

Folk, R. L. & Ward, W. C. 1957. Brazos river bar: a study in the signifiance of grain size parameters. J. Sedim. Petrol. 27: 3-26.

Gerlach, D. C., Frey, F. A., Moreno-Roa, H., and Lopez-Escobar, L., 1988. Recent volcanism in the Puyehue-Cordon Caulle Region, Southern Andes, Chile (40.5°S): Petrogenesis of evolved lavas. J. Petrol. 29: 333-382.

Glasser N.F., Harisson S., Winchester V. and Aniya M. 2004. Late Pleistocene and Holocene palaeoclimate and glacier fluctuations in Patagonia. Glob. Plan. Change 43: 79-101.

Grootes, P. M., Stuiver, M., White, J. W. C., Johnsen, S. & Jouzel, J. 1993. Comparison of oxygen isotope records from the GISP2 and GRIP Greenland ice cores. Nature 366: 552-554.

Grosjean M., Geyh M.A., Messerli B., Schreier H. and Veit H. 1998. A late-Holocene (<2600 BP) glacial advance in the south-central Andes (29°S), northern Chile. The Holocene 8(4): 473-479.

Hajdas I., Bonani G., Moreno P. and Aritzegui D. 2003. Precise radiocarbon dating of Late-Glacial cooling in mid-latitude South America. Quat. Res. 59: 70-78.

Heiri O., Lotter A.F. and Lemcke G. 2001. Loss on ignition as a method for estimating organic and carbonate content in sediments: reproductibility and comparability of results. J. Paleolim. 25: 101-110.

Heusser C.J. 1990. Chilotan piedmont glacier in the Southern Andes during the Last Glacial Maximum. Rev Geol. Chile 17: 3-18.

Heusser C.J. 2003. Ice age Southern Andes - A chronicle of palaeoecological events. Elsevier, Amsterdam, 230 pp.

Heusser C.J., Heusser L.E. and Lowell T.V. 1999. Paleoecology of the southern Chilean Lake District-Isla Grande de Chiloé during middle-late Llanquihue glaciation and deglaciation. Geog. Ann. 81 A(2): 231-284.

Heusser C.J., Lowell T.V., Heusser L.E., Hauser A., Andersen B.G. and Denton G.H. 1996. Full-glacial - late-glacial palaeoclimate of the Southern Andes: evidences from pollen, beetle and glacial records. J. Quat. Sci. 11: 173-184.

Jenny B., Valero-Garcés B.L., Villa-Martínez R., Urrutia R., Geyh M. and Veit H. 2002. Early to Mid-Holocene aridity in Central Chile and the Southern Westerlies: the laguna Acuelo record (34°S). Quat. Res. 58: 160-170.

Johnson T.C., Brown E.T., McManus J., Barry S.L., Barker P. and Gasse F. 2002. A high-resolution paleoclimate record spanning the past 25,000 years in Southern East Africa. Science 296: 113-114, 131-132.

Knorr G. and Lohmann G. 2003. Southern Ocean origin for the resumption of Atlantic thermohaline circulation during deglaciation. Nature 424: 532-536.

Lamy F., Hebbeln D., Röhl U. and Wefer G. 2001. Holocene rainfall variability in southern Chile: a marine record of latitudinal shifts of the Southern Westerlies. Earth Plan. Sci. Let. 185: 369-382.

Lamy F., Kaiser J., Ninnemann U., Hebbeln D., Arz H.W. and Stoner J. 2004. Antarctic timing of surface water changes off Chile and Patagonian ice sheet response. Science 304: 1959-1962.

Lamy F., Rühlemann D., Hebbeln D. and Wefer G. 2002. High- and low-latitude climate control on the position of the southern Peru-Chile Current during the Holocene. Paleoceanography 17: 1028, doi:10.1029/2001PA000727.

Laugenie C. 1982. La région des lacs, Chili méridional. Unpublished PhD thesis, Université de Bordeaux III, 822 p.

Leinen M. 1977. A normative calculation technique for determining opal in deep-sea sediments. Geochim. Cosmochim. Acta 41: 671-676.

Lotter A.F., Birks H.J.B. and Zolitschka B. 1995. Late-glacial pollen and diatom changes in response to two different environmental perturbations: volcanic eruption and Younger Dryas cooling. J. Paleolim. 14: 23-47.

Lowell T.V., Heusser C.J., Andersen B.G., Moreno P.I., Hauser A., Heusser L.E., Schlüter C., Marchant D.R. and Denton G.H. 1995. Interhemispheric correlation of Late Pleistocene glacial events. Science 269: 1541-1549.

McCulloh R.D., Bentley M.J., Purves R.S., Hulton N.R.J., Sugden D.E. and Clapperton C.M. 2000. Climatic inferences from glacial and palaeoecological evidence at the last glacial termination, southern South America. J. Quat. Sci. 15: 409-417.

Mercer J.H. 1972. Chilean glacial chronology 20,000 to 11,000 caron-14 years ago: some global comparisons. Science 176: 1118-1120.

Miller A. 1976. The climate of Chile. In: Schwerdtfeger W, editor. World survey of Climatology. Elsevier, Amsterdam, pp. 107-134.

Moore D.M. and Reynolds R.C.J. 1989. X-ray diffraction and the identification and analysis of clay minerals. Oxford University Press, 332 p.

Moreno P.I. 1997. Vegetation and climate near Lago Llanquihue in the Chilean Lake District between 20200 and 9500 ^{14}C yr BP. J. Quat. Sci. 12: 485-500.

Moreno P.I. 2000. Climate, Fire, and Vegetation between About 13,000 and 9200 ^{14}C yr B.P. in the Chilean Lake District. Quat. Res. 54: 81-89.

Moreno P.I. 2004. Millenial-scale climate variability in northwest Patagonia over the last 15000 yr. J. Quat. Sci. 19: 35-47.

Moreno P.I., Jacobson G.L.J., Lowell T.V. and Denton G.H. 2001. Interhemispheric climate links revealed by a late-glacial cooling episode in southern Chile. Nature 409: 804-808.

Moreno P.I. and Leon A.L. 2003. Abrupt vegetation changes during the last glacial to Holocene transition in mid-latitude South America. J. Quat. Sci. 18: 1-14.

Moreno P.I., Lowell T.V., Jacobson G.L.J. and Denton G.H. 1999. Abrupt vegetation and climate changes during the last glacial maximum and last termination in the Chilean Lake District: a case study from Canal de la Puntilla (41°S). Geog. Ann. 81 A(2): 285-311.

Muñoz M. 1980 Flora del parque nacional Puyehue. Universitaria, Santiago, 557 p.

Parada M.G. 1973. Pluviometria de Chile. Isoyetas de Valdivia-Puerto Montt. CORFO Departamento de Recursos hydraulicos. 73 p.

Sterken, M., Verleyen, E., Sabbe, K., De Batist, M. & Vyverman, W. 2006a. The effect of tephra depositions on diatom productivity and composition in Lago Puyehue, southern Chile. J. Paleolimnol.

Sterken M., Verleyen E., Sabbe K., Terryn G., Charlet F., Bertrand S., Boës X., Fagel N., De Batist M. & Vyverman W. 2006b. Late Quaternary climatic changes in southern Chile, as recorded in a diatom sequence of Lago Puyehue (40°40' S). J. Paleolimnol.

Stuiver M., Reimer P.J., Bard E., Beck J.W., Burr G.S., Hughen K.A., Kromer B., McCormac G., van der Plicht J. and Spurk M. 1998. Intcal98 radiocarbon age calibration, 24,000-0 cal BP. Radiocarbon 40: 1041-1083.

van Geel B., Buurman J. and Waterbolk H.T. 1996. Archaeological and paleoecological indications of an abrupt climate change in The Netherlands, and evidence for climatological teleconnections around 2650 BP. J. Quat. Sci. 11: 451-460.

van Geel B., Heusser C.J., Renssen H. and Schuurmans C.J.E. 2000. Climate change in Chile at around 2700 BP and global evidence for solar forcing: a hypothesis. The Holocene 10: 659-664.

van Geel B. and Renssen H. 1998. Abrupt climate change around 2,650 BP in North-West Europe: evidence for climatic teleconnections and a tentative explanation. In: Issar A, Brown N (eds). Water, environment and society in times of climatic change. Kluwer, Dordrecht, pp. 21-41.

Vargas L., Roche E., Gerrienne P. and Hooghiemstra, H. 2006. Pollen-based record of Lateglacial-Holocene climatic variability on southern Lake District, Chile. J. Paleolimnol.

Zimmerman A.R. and Canuel E.A. 2002. Sediment geochemical records of eutrophication in the mesohaline Cheasapeake Bay. Limn. Ocean. 47: 1084-1093.

Table 1: AMS radiocarbon dates obtained on bulk sediment of PU-II long core. The range of calendar ages is calculated with OxCal v3.9 (Bronk Ramsey 2001). The weighted average is calculated with BCal and used for age-depth modelling. The two dates at 2570 and 2590 ^{14}C yr. BP are located in an important plateau of the radiocarbon calibration curve. For that period, three hundred ^{14}C years correspond to 90 calendar years (van Geel et al. 1996).

Depth (mblf)	Laboratory n°	^{14}C age +- 1σ (yr BP)	2σ error range calibrated ages (OxCal) (cal yr BP)	Weighted Average (BCal) (cal yr BP)
120.5 cm	Poz-5922	2570 ± 35	2490 - 2770 (95.4 %)	2655
156.5 cm	Poz-1406	2590 ± 40	2490 - 2790 (95.4 %)	2681
306.5 cm	Poz-7660	4110 ± 40	4510 - 4830 (92.7 %)	4648
400.5 cm	Poz-2201	5300 ± 40	5940 - 6200 (95.4 %)	6074
463.75 cm	Poz-5923	5760 ± 40	6440 - 6670 (95.4 %)	6560
627.75 cm	Poz-5925	7450 ± 50	8160 - 8390 (93.9 %)	8262
762 cm	Poz-1405	10010 ± 60	11200 - 11750 (91.0 %)	11494
908 cm	Poz-7661	11440 ± 80	13100 - 13850 (95.4 %)	13407
1012 cm	Poz-2215	13410 ± 100	15250 - 16750 (95.4 %)	16063
1119 cm	Poz-7662	12880 ± 90	14350 - 15950 (95.4 %)	15355

Table 2: Correlation coefficients between the different proxies measured on PU-II long core sediments. MS = magnetic susceptibility and GS = grain size.

LOI_{105}	1						
LOI_{550}	0.89	1					
bio-SiO_2	0.75	0.62	1				
TiO_2	-0.70	-0.71	-0.74	1			
Al_2O_3	-0.74	-0.59	-0.99	0.68	1		
MS	-0.58	-0.47	-0.53	0.37	0.53	1	
Mean GS	0.79	0.67	0.71	-0.69	-0.72	-0.46	1
	LOI_{105}	LOI_{550}	bio-SiO_2	TiO_2	Al_2O_3	MS	Mean GS

Figure captions

Figure 1: Location of Lago Puyehue among the Chilean Lake District. PU-II coring site has been selected after a seismic investigation of the lake sedimentary infill (Charlet et al. 2006) and is indicated on the bathymetric map of Lago Puyehue (Campos et al. 1989). Isobath = 20 m.

Figure 2: Schema of correlations between the 3m long sections for the realisation of the composite core. The composite log is drawn according to macroscopical descriptions.

Figure 3: Age-depth model constructed by 4 linear regressions. Mean weighted average calibrated ages were used. Error bars represent the range of calibrated radiocarbon ages (see Table 1). Linear regressions were realised with psimpoll software (Bennett, 1994).

Figure 4: Mineralogy and physical parameters of PU-II long core. Magnetic susceptibility results are represented with a 9 points running average. Grain size results are represented with a 9 (0-430 cm) or 3 (430-1120 cm) points running average in order to represent a similar sampling step. Data associated with tephra layers were removed from the database. For mineralogical semi-quantification, the intensity of the principal peak of each mineral was measured and corrected by a multiplication factor from Cook et al. (1975). For amorphous material, a mean correction factor was obtained from diffraction results on mixtures of known quantities of amorphous material and quartz. We calculated a mean correction factor of 75, applied to the maximum of the broad diffraction band at 3.7 Å. The vermiculite content is estimated from the intensity of the (001) diffraction peak at 14.5 Å. The grey shaded rectangles underlay a turbidite between 956 and 971 cm.

Figure 5: Al_2O_3 and TiO_2 weight percentages measured on PU-II long core. Bio-SiO_2 weight percentage is estimated by normative calculation assuming a constant SiO_2/Al_2O_3 ratio for the detrital source (3.5). The grey shaded rectangles underlay a turbidite between 956 and 971 cm.

Figure 6: Results of the principal component analysis realised on the physical and geochemical variables measured on PU-II long core. The X axis explains 71.61 % of the variability and the analysis clearly demonstrates 2 groups of data: 1) LOI_{105}, LOI_{550}, bio-SiO_2 and Mean G.S and 2) TiO_2, Al_2O_3 and magnetic susceptibility. MS = magnetic susceptibility and GS = grain size.

Figure 7: Grain size distribution of a typical PU-II sediment sample (example at 70.5 cm). The grain size distribution has been measured on bulk sample and after dissolution of biogenic silica and organic matter by Na_2CO_3 and H_2O_2. The detrital grain size distribution has been calculated by difference.

Figure 8: Sediment composition changes as a function of time. Mass Accumulation Rates (MAR) of biogenic silica and terrigenous particles are calculated for the period before 9000 cal yr BP, where the age-depth model does not present breakpoints. For MAR calculation, dry density deduced from gamma density data corrected from water content has been used (see Bertrand et al. 2005). MAR in $g \cdot m^2/yr$. Grey densities on the right of the figure represent interpretations of temperature. The denser colour, the warmer the climate is.

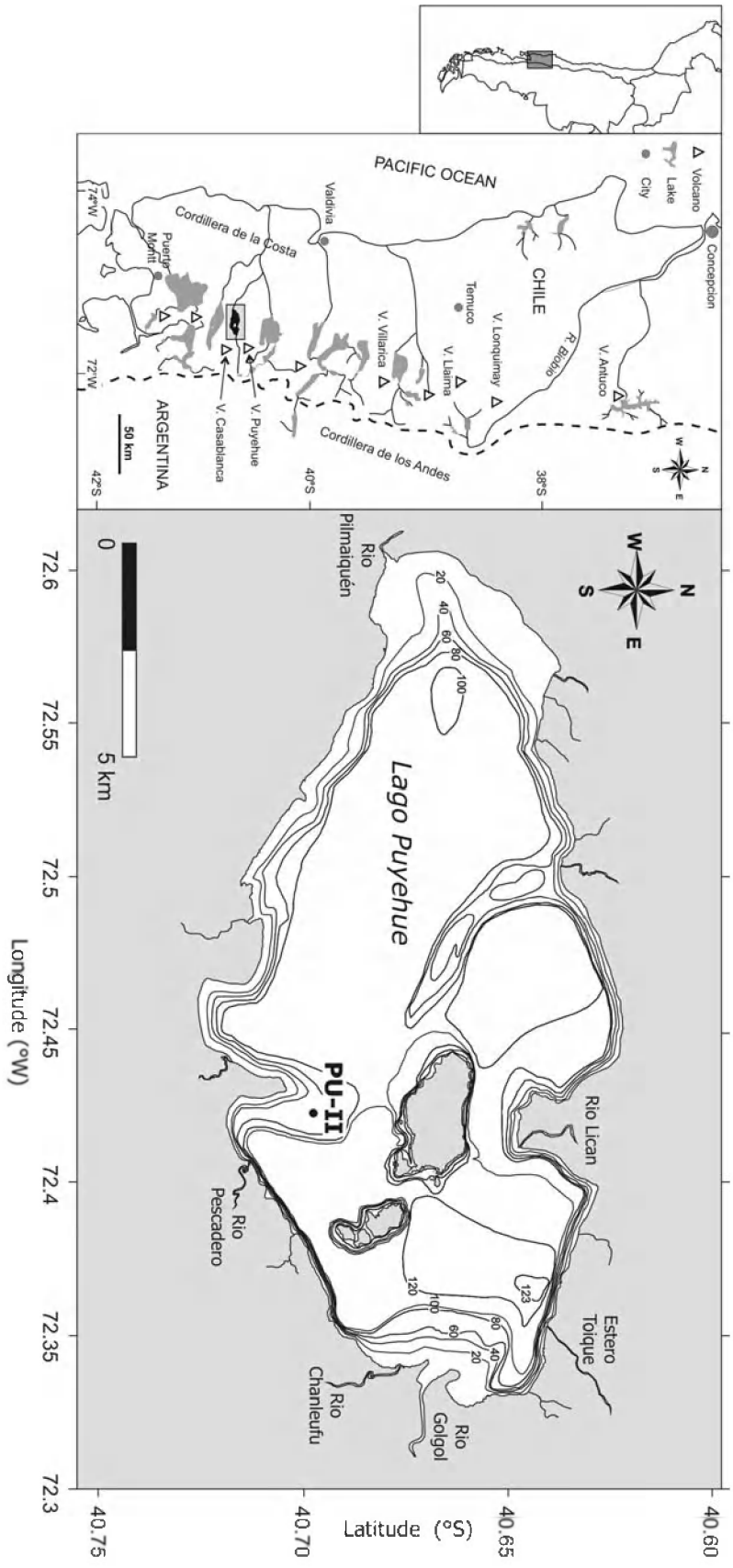

Bertrand et al – Figure 1

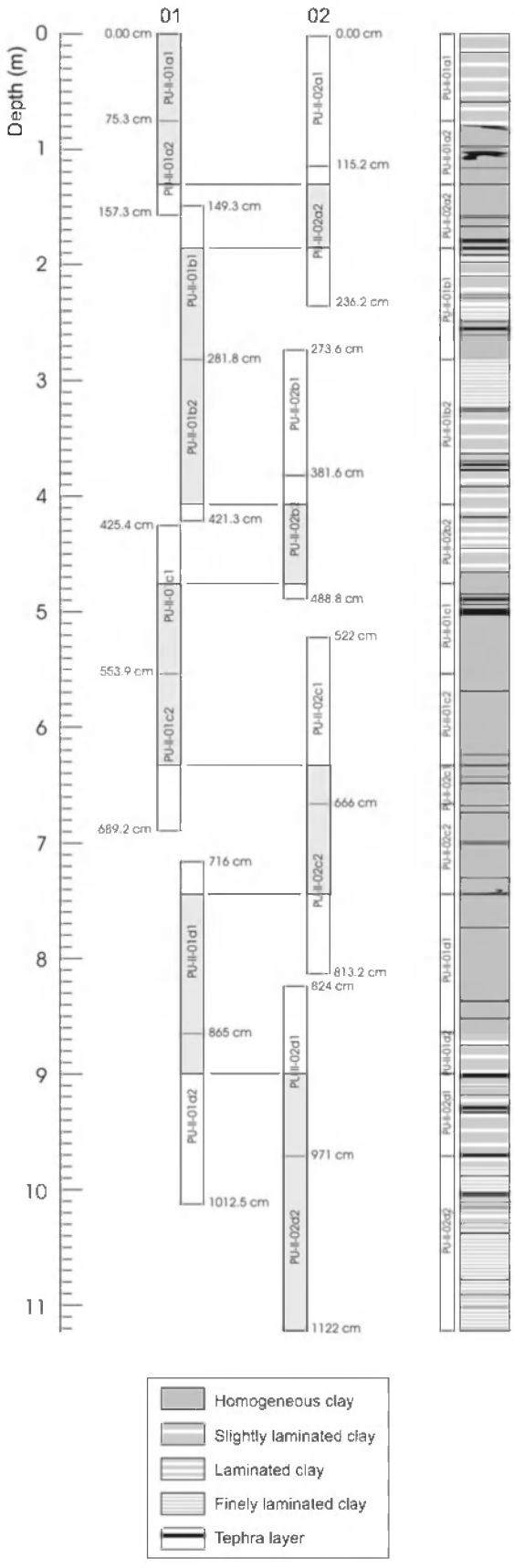

Bertrand et al – Figure 2

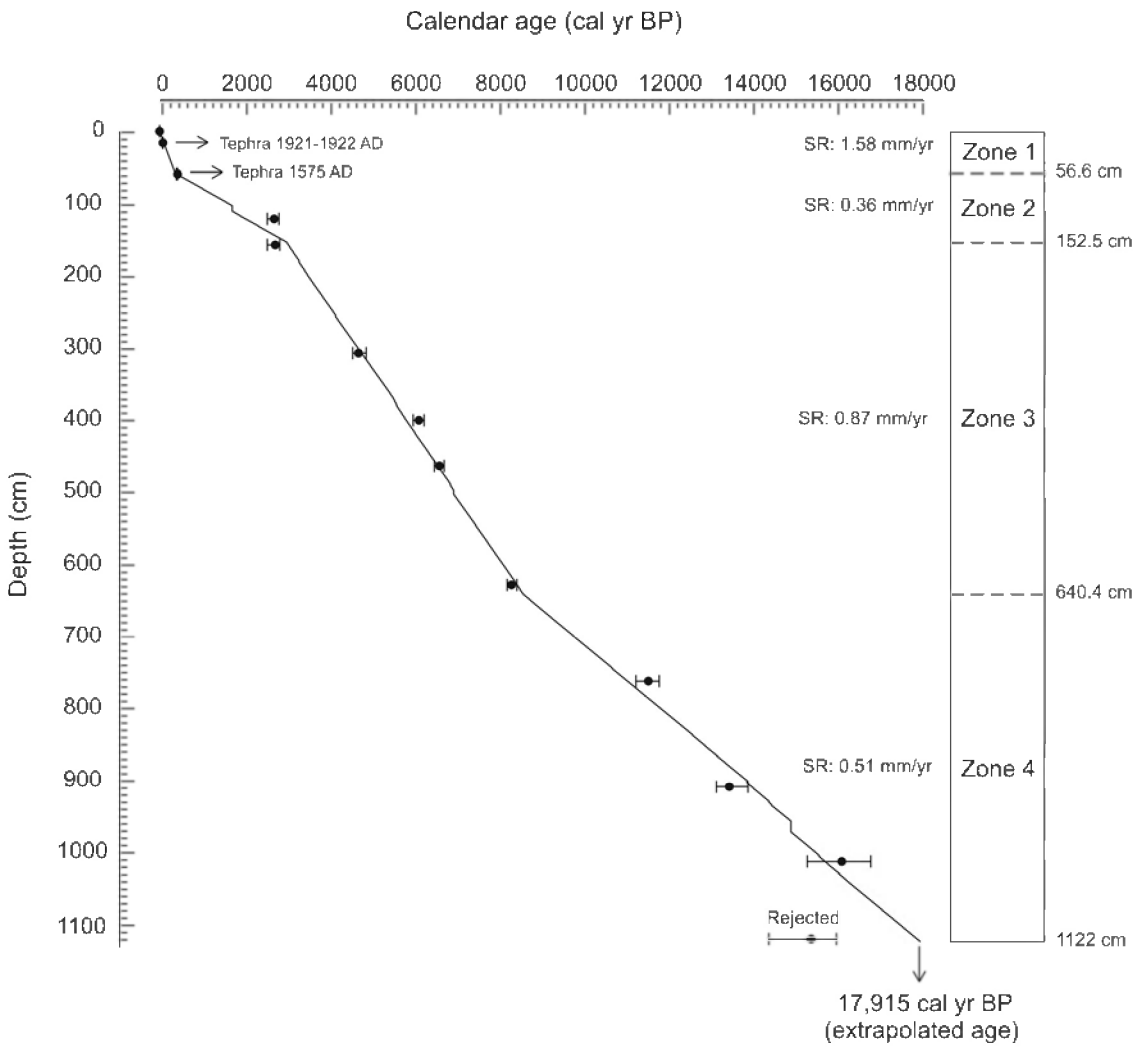

Bertrand et al – Figure 3

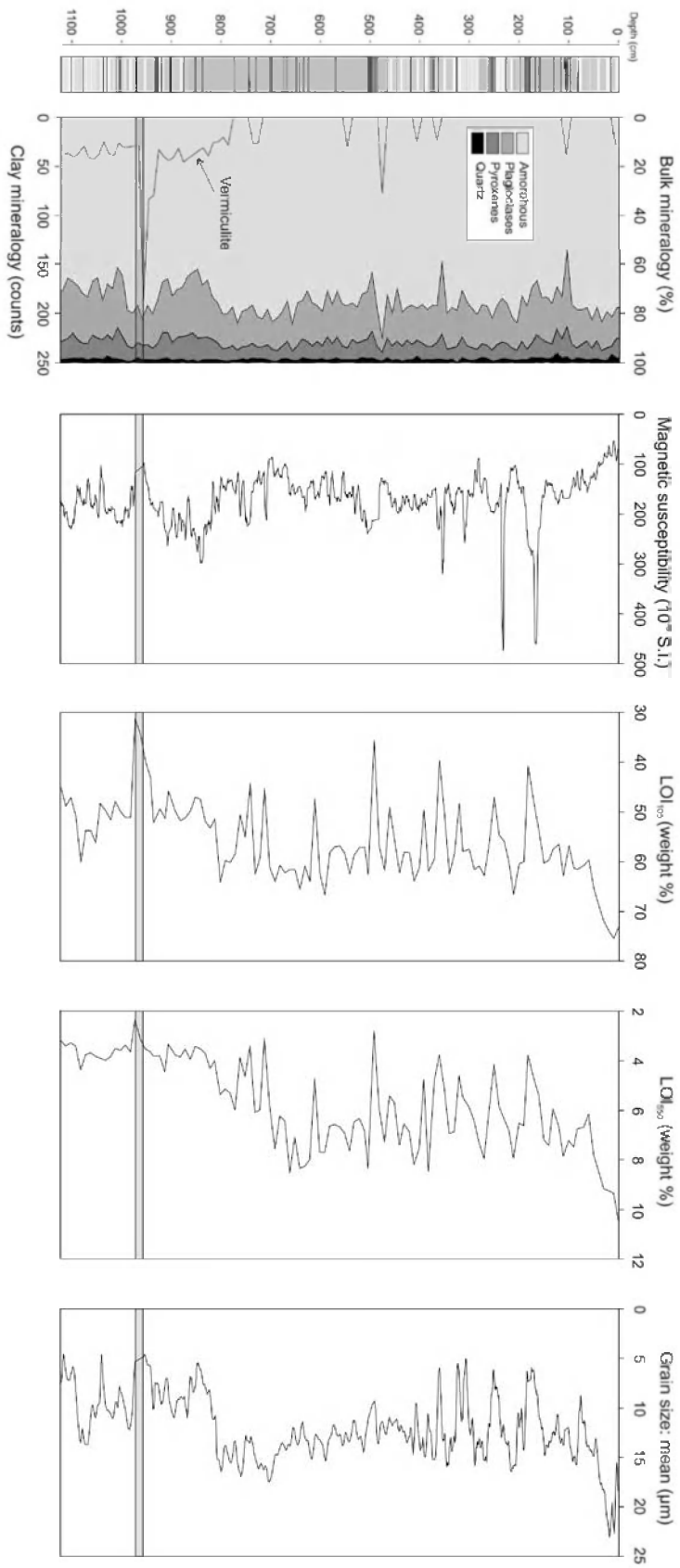

Bertrand et al – Figure 4

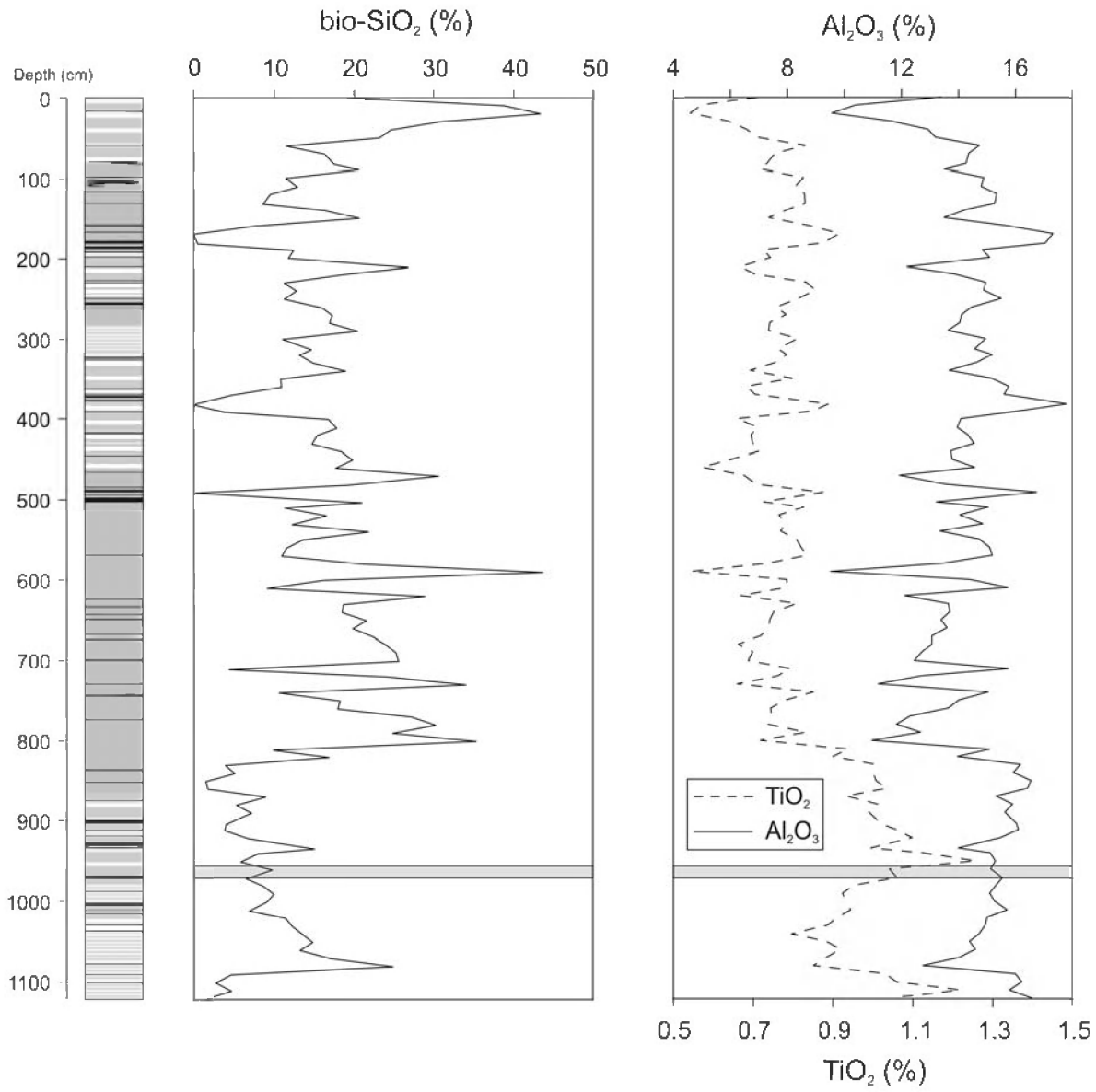

Bertrand et al – Figure 5

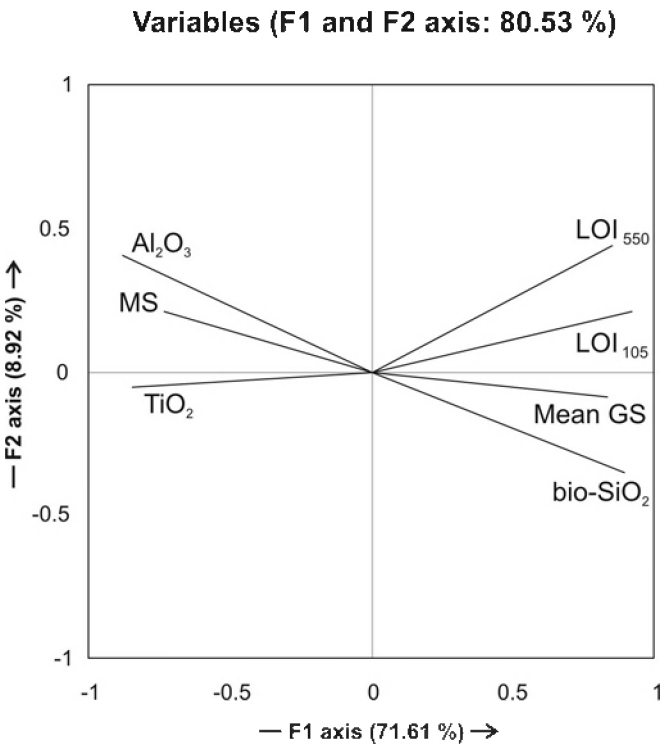

Bertrand et al – Figure 6

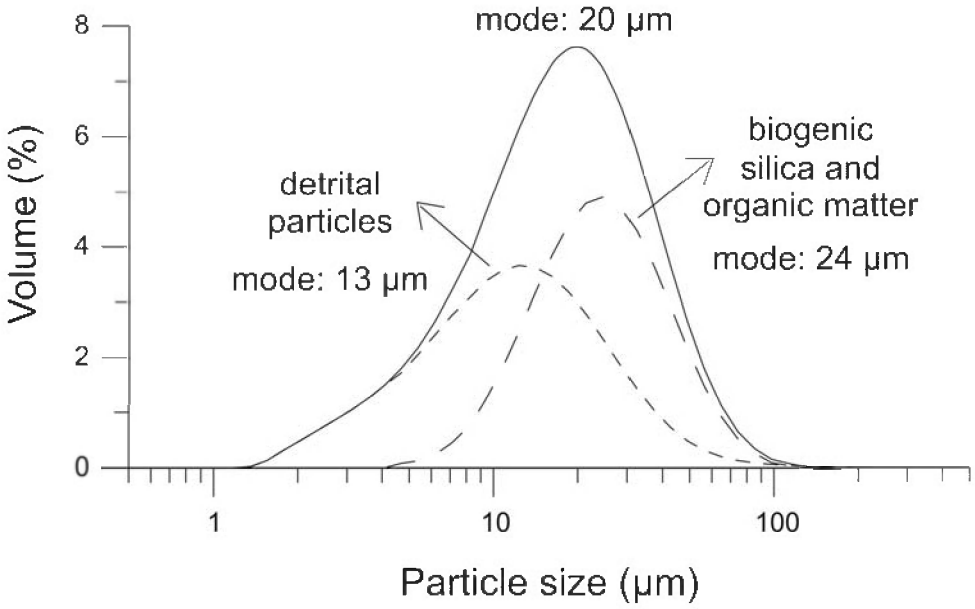

Bertrand et al – Figure 7

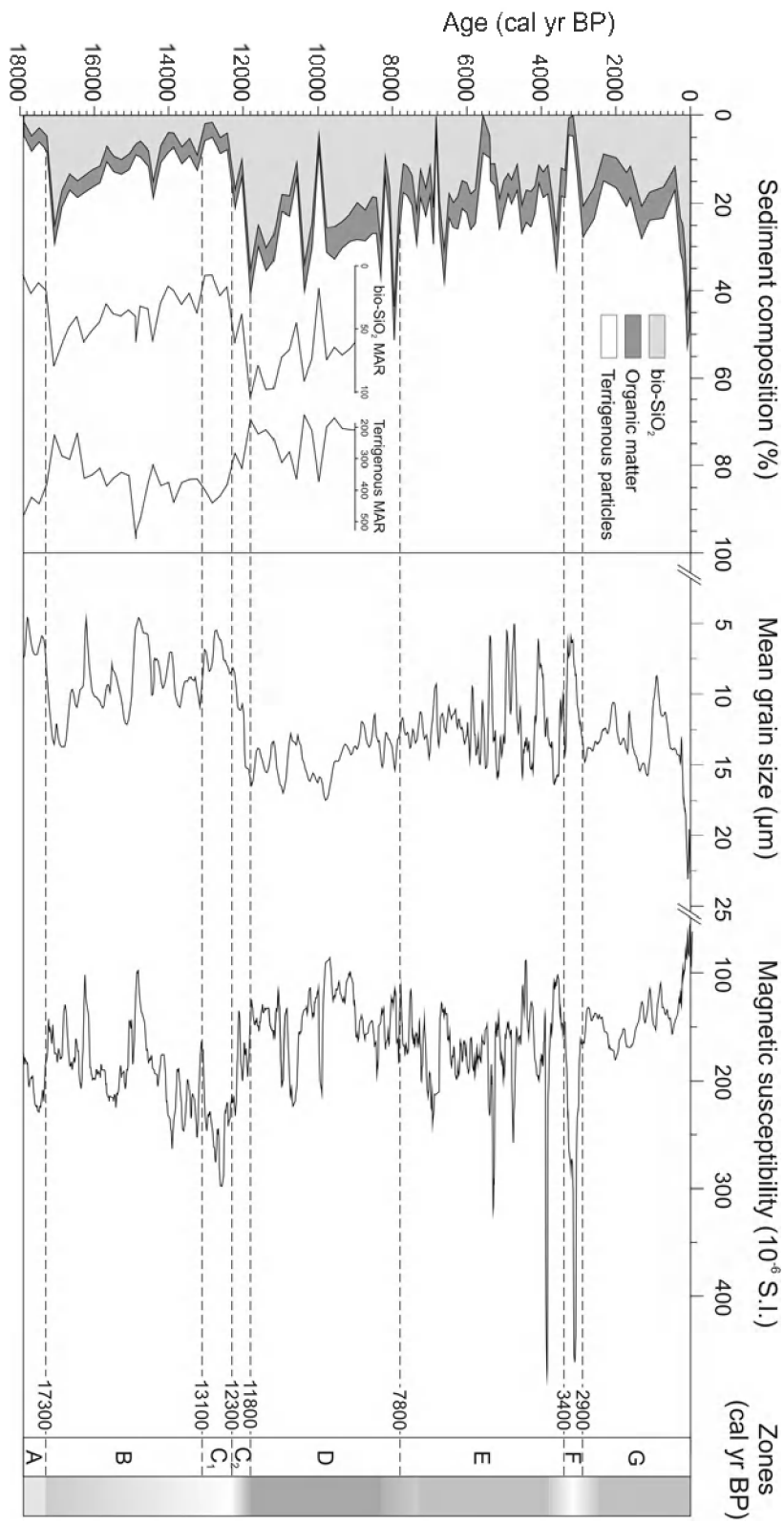

Bertrand et al – Figure 8